PRAMANA
— journal of
physics

Vol. 41, No. 3,
September 1993
pp. 271–283

A translational energy spectrometer to probe interatomic potentials: Dissociation dynamics of CO_2^+ ions

M KRISHNAMURTHY, U T RAHEJA and D MATHUR
Atomic and Molecular Sciences Laboratory, Tata Institute of Fundamental Research, Homi Bhabha Road, Bombay 400 005, India

MS received 28 April 1993

Abstract. A new ion translational energy spectrometer has been developed to carry out low-energy, gas-phase ion-molecule collision experiments which aim to probe molecular potential energy surfaces. The collisional technique employed relates small changes in the kinetic energy of a projectile ion after it has undergone collision with a static neutral atom/molecule to changes in the overall potential energy of the collision system; information can be furnished about the interaction potential between the projectile and the target. First measurements are reported of a high resolution target excitation spectrum obtained in 1.8 keV collisions of H_2^+ ions with N_2. New results pertaining to collision-induced dissociation of CO_2^+ ions are presented and discussed in terms of potential functions of low-lying electronic states of the molecular ion.

Keywords. Ion-molecule collisions; translational energy spectrometer; dissociation; energy loss spectra.

PACS Nos 35·80; 34·50

1. Introduction

Quantitative insight into interatomic potentials which govern the dynamics of chemical transformation processes continues to elude physicists and chemists. Despite many far-reaching strides that have been made in development of experimental techniques in the course of the last decade, an active need continues to be felt to develop new methodologies for investigating the *dynamical* aspects of chemical transformation processes on a microscopic level, *collision by collision.* Ion translational energy spectrometry (TES) is an example of one such recent development. TES is a gas-phase collisional technique in which analysis of the changes in the kinetic energy of a projectile ion which has undergone collision with a neutral target atom or molecule furnishes information about the interaction potential between the projectile and the target. When the projectile is a charged species, ion-neutral reactions can be investigated whose dynamics are dominated by interactions which occur at large internuclear distances. In other words, only the long-range part of the overall potential energy surface on which a given reaction occurs need be considered in concomitant theoretical studies. This provides a distinct advantage insofar as quantitative understanding of reaction dynamics needs theoretical information of only a subset of the entire complex interatomic potential surface; conversely, experimental results forthcoming from TES measurements of ion-neutral reaction phenomena provide a stringent test of the effectiveness of contemporary quantal techniques of generating molecular potential energy surfaces.

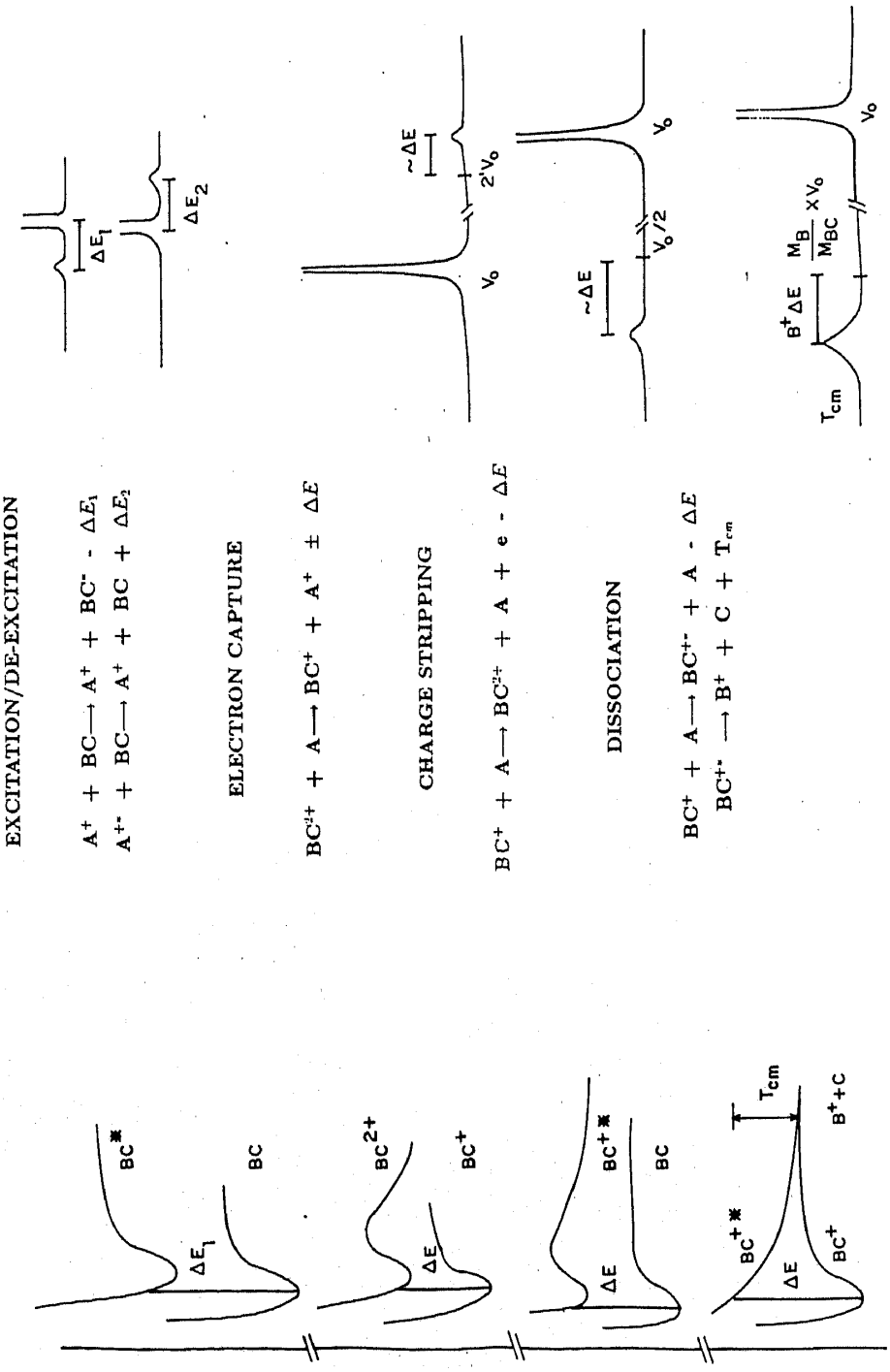

Figure 1. A summary of different ion-neutral collision processes that are assessible to translational energy spectrometry. The relationship of each collision process to transitions between different molecular potential energy curves is illustrated on the left side of the figure; the right side is a schematic representation of how each transition would manifest itself in the ion translation energy spectrum (V_0 represents the elastically scattered ion peak in all cases, and ΔE is the energy defect associated with each process.)

Translational energy spectrometer

We describe here the development of a new, high-sensitivity, high-resolution, multi-sector ion translational energy spectrometer which is used to carry out experimental studies of atomic collision processes, particularly those involving low-energy, single collisions between gas-phase positive ions and neutral atoms or molecules. An entire gamut of reaction dynamics can be studied using our apparatus (see refs. [1, 2] for recent reviews of the application of the TES technique to experimental studies of molecular structure and dynamics). Figure 1 illustrates processes leading to single and multiple electron capture, charge stripping and dissociation; these provide examples of ion-neutral reactions which occur readily at large internuclear separations of reactant species and which are amenable to interpretation in terms of molecular potential energy functions which can be computed using contemporary ab initio molecular orbital techniques.

We present below details of our TES apparatus as well as new results on the dynamics of collision-induced dissociation of CO_2^+ ions. Apart from its significance to atmospheric chemistry and laser plasma physics, dissociation of CO_2^+ ions, leading to formation of $O^+ + CO$ or $CO^+ + O$ fragments, is of fundamental importance. The former fragmentation channel would be expected to be energetically favoured. However, our results indicate that the signal corresponding to the $CO^+ + O$ channel is several factors larger in intensity than the $O^+ + CO$ channel. Furthermore, contemporary quantum-mechanical wisdom does not permit the formation of either of the two fragment channels by direct dissociation of low-lying bound $X^2\Pi_g$, $A^2\Pi_u$ or $B^2\Sigma_u^+$ electronic states of CO_2^+ since the respective dissociation continua cannot be accessed via vertical, Franck–Condon transitions from the ground electronic state of CO_2. We interpret our results in terms of a curve-crossing picture involving excited electronic states of CO_2^+ in which the apparent suppression of the lowest-energy pathway to dissociation is accounted for.

2. Translational energy spectrometer

TES involves the determination of the energetics of a single collision reaction between a projectile ion and a target atom or molecule. When a monoenergetic beam of mass-selected projectile ions interacts with the neutral target, the energy balance of the reaction manifests itself as changes in the translational energy of the projectile ions under kinematic conditions of fast collision and forward scattering (large impact parameter collisions with nearly zero momentum transfer). The technique, therefore, requires formation of a monoenergetic beam of the appropriate ionic species and known translational energy, its interaction with a neutral gas target under conditions which ensure that only a single collision occurs (ultra high vacuum conditions leading to mean-free-paths which are very much larger than the dimensions of the apparatus). The post-collision translational energy has to be measured at zero degrees scattering angle with an adequate energy resolution. A schematic diagram of our TES apparatus which incorporates all these requirements is shown in figure 2.

The projectile ions in our apparatus are produced in a low pressure (*ca.* 10^{-6} torr) ion source with electrons of 70–100 eV energy. The ions formed in a field-free region are extracted by an electrostatic potential of 1·5–5 kV and focussed into a fine pencil beam by a three-element cylindrical einzel lens system. This beam then enters a region of crossed electric and magnetic fields (Wien filter), where momentum selection occurs. A suitable m/q of particles may be selected by suitably balancing the forces due to electric and magnetic fields in opposite directions. Mass selected ions are then energy

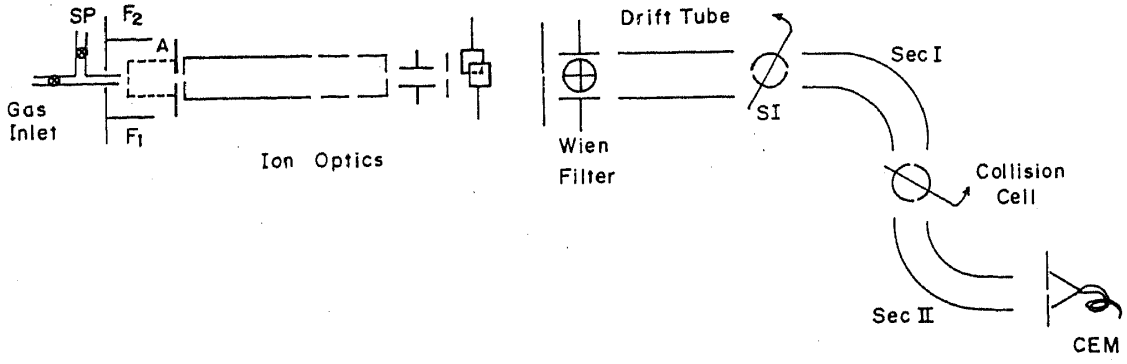

Figure 2. Schematic diagram of the ion translational energy spectrometer. $F_{1,2}$ and A are the two tungsten filaments and anode, respectively, which comprise the electron impact ion source; SI defines the entry slit into the first electrostatic energy analyser (Sec I); the rotating collision cell provides a continuously adjustable slit which acts as the entrance to the second energy analyser (Sec II); CEM is the channel electron multiplier detector. Details of the mechanical design of individual components are available from the authors.

monochromatized by a 90° cylindrical sector electrostatic analyser of mean radius 55 cm. The monoenergetic ions are then made to interact with a neutral gas target in a collision cell maintained at about 5×10^{-6} torr with gas load. The product ions formed in the projectile beam are energy analysed by a second, identical 90° electrostatic analyser. Ion detection is by a channel electron multiplier operating in the particle counting mode, coupled to conventional pulse counting electronics and a computerised data acquisition system. The overall background pressure in the apparatus is maintained in the 1×10^{-7} torr region; differential pumping is achieved by means of four oil diffusion pumps and one ion pump.

The sizes of the entry and the exit slits of the 90° cylindrical sector electrostatic analyser determine the energy resolution that can be obtained. We have designed variable width slits, whose widths can be varied on-line from 0 mm to about 1 mm. Taken together with the large radius of our energy analysers, our instrument is capable of energy resolving powers in excess of 2×10^4 in the laboratory frame. In the case of dissociation studies of the type reported below, the effective resolving power obtainable in the centre-of-mass frame is several orders of magnitude larger. Indeed, the TES technique has been utilized by us to study rotational resonances in ion-molecule collisions using another, lower-resolution apparatus in our laboratory [3,4].

The total distance that an ion traverses from the ion source to the detector in the apparatus is of the order of 3 m.

2.1 *Ion injection system*

Electrons from a peripherally positioned hot thoriated tungsten filament are accelerated by a hollow cylindrical mesh anode to enter the field-free region perpendicular to the anode axis. The electron energy can be varied up to 500 eV. A gas jet is positioned along the anode axis. Ions are formed by electron impact ionization in the field-free region and are formed in the ground state as well as the excited states. The major advantages of this ion source lies in its stability and its simplicity.

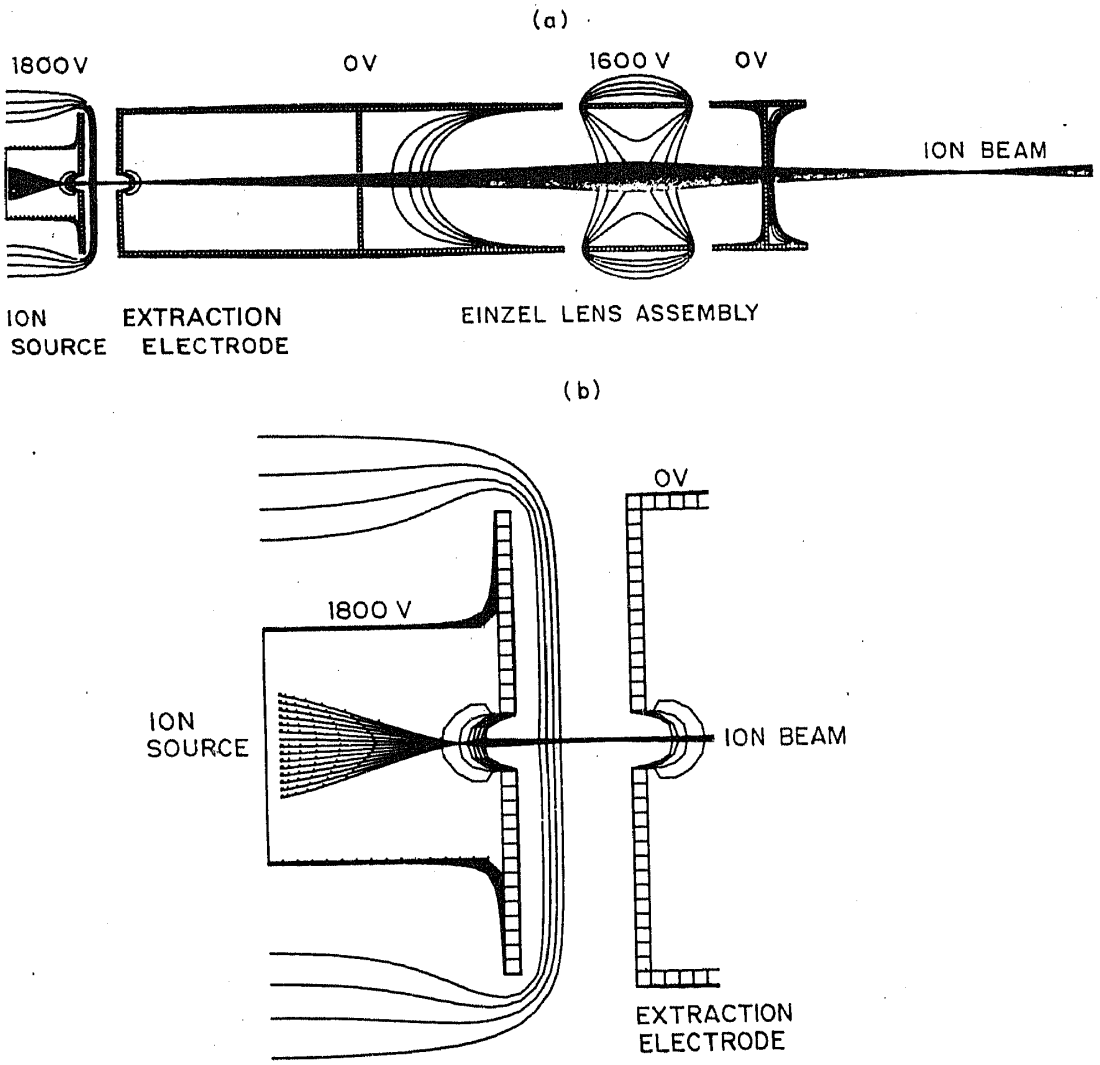

Figure 3(a). Computer simulations of N_2^+ ion (1·8 keV energy) trajectories in the ion source, extraction and focussing system. **(b).** Expanded view of ion extraction from the ion source by a penetrating field. The dotted contours intersecting the ion beam trajectory within the source region represent ion transit time periods of 2 μs each; a typical residence time for N_2^+ ions within the source is estimated to be *ca* 16 μs.

Ions formed in the field free region are extracted by an electric field penetrating through a fine anode aperture. The field penetration into the anode mesh determines the energy spread in the extracted ion beam. In our design, considerable effort was expended to minimize the field penetration into the anode mesh by making the anode aperture smaller whilst, at the same time, ensuring that the efficiency of ion extraction is not reduced to unmanageable proportions. Figure 3 illustrates the field penetration pattern and the ion extraction efficiency of the optimised configuration that we arrived at after a large number of computer simulations were carried out using the ion trajectory method of Dahl *et al* [5] in the following manner.

The region of interest in the apparatus was notionally covered with a cartesian grid of points. Laplace's equation for the appropriate geometry, together with a Taylor series expansion of the potential at every adjacent point, is utilized to express the potential at an arbitrary point in the array in terms of the potential at the

surrounding points. The grid points which correspond to ion source and extraction electrodes are held at the desired voltages, and the potential of each free point is calculated in terms of the surrounding points. Repeated iterations are performed; monitoring the change in potential at a point after each cycle shows when an adequate level of convergence has been achieved. Upon calculations of the potential array to a satisfactory degree of accuracy, the trajectories of a large number of ions in that field are calculated by numerical integration of the equations of motion for given initial position and velocity. The actual electrostatic field calculations is by means of the finite difference relaxation method [6].

In figure 3(b) we also show the results of calculations which offer an indication of the amount of time that molecular ions, of the type used in subsequent studies to be described below, take to traverse the ion source prior to extraction. The dotted lines shown within the ion source region indicate time separations of 2 μs. In the actual example shown in the figure N_2^+ ions, formed initially with only thermal energy, traverse through the source in a time period of about 16 μs. If the gas pressure within the source is sufficiently high, it may be possible to use the ion transit time information to deduce the degree of collisional de-excitation of the incident ion beam as it emerges from the source. Further work on this aspect of our design is under way.

Ions are electrostatically extracted by an accelerating potential of about 1–5 kV; the extracted ions are focussed by a three-element einzel lens system, whose design is identical to the one used in standard TV tube guns. The ion beam, further collimated mechanically by a fine aperture, enters a crossed electric and magnetic field analyser where the desired mass-to-charge (m/q) ratio of ions on the axis is selected by suitably balancing the forces exerted by the electric and magnetic fields in opposite directions.

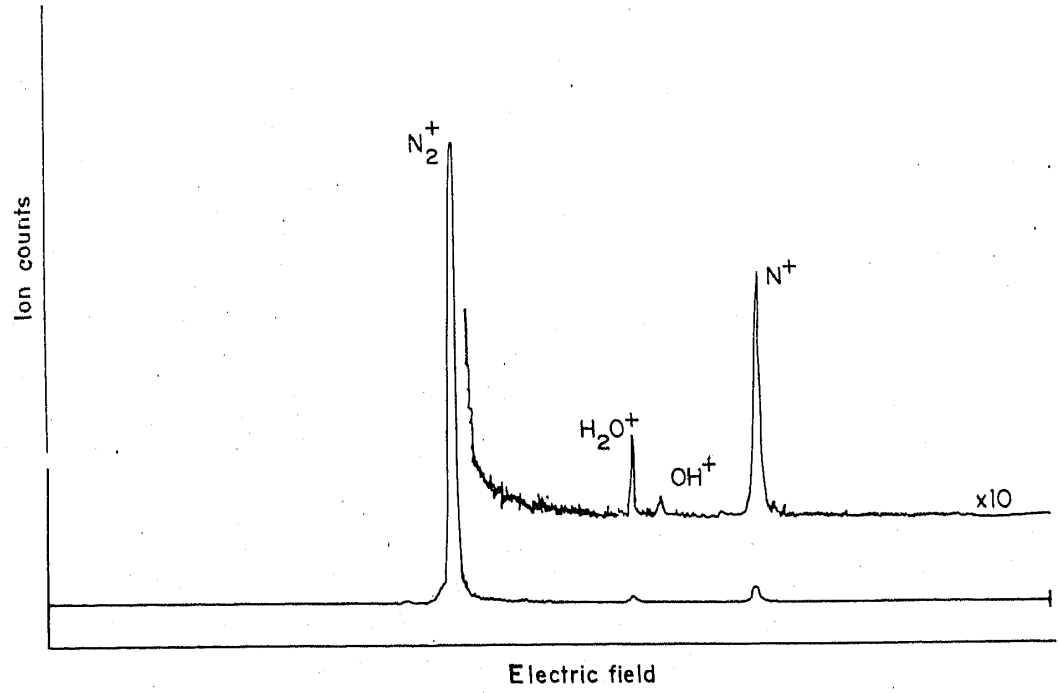

Figure 4. Typical mass spectrum obtained under focussing conditions such that unit mass resolution is obtained when a mixture of N_2 and H_2O are introduced into the ion source. The spectrum was obtained by varying the Wien filter's electric field over the range from 0 to 56 V cm^{-1} and keeping the magnetic field constant at 300 G.

Translational energy spectrometer

The crossed field analyser used in the present apparatus is identical to that used in an earlier apparatus in our laboratory [7,8] and will not be described here. It is, however, pertinent to point out the simple manner in which this device enables the mass resolution (and, correspondingly, the intensity of the ion signal that is transmitted) to be optimized for a given experimental situation by suitable choice of either electric field or magnetic field. A typical mass spectrum is shown in figure 4, illustrating unit mass resolution, which is more than adequate for the type of collision induced dissociation experiment which we report below.

2.2 *Energy monochromation and analysis*

The kinetic energy of the incident ion beam and post-collision energy analysis are both accomplished by means of two, large cylindrical electrostatic analysers. Both analysers are identical and consist of 55 cm mean radius 90° sectors with 2·0 cm radial gap. Factory-polished stainless steel sheets coated with colloidal graphite (to reduce surface space charge effects) are placed in 90° precision grooved holders on the top and bottom. Each analyser is assembled with the help of jigs to ensure the required gap, mean radius, parallelity, concentricity and exact 90° sector angle. There are locking devices incorporated which lock the sector assembly and prevent it from changing position when the jigs are dispensed with. The positions of all the mechanical fittings and supports for the sector elements inside each vacuum chamber are ensured by a right angle jig as the vacuum chamber (which consists of five segments) and the end flanges are welded with the jig and analyser assembly in the required position. Thus, all the critical parameters of mechanical design are kept under control and within the desired range by use of jigs throughout the fabrication and subsequent re-assembly stages.

The housing for the inter-sector slits also incorporates the gas target; by providing a gas flow in the variable sit assembly used in the present apparatus, the inter-sector slit has been converted into a gas target-cum-variable slit. The target region requires fast differential pumping. The position of the slits is dictated by the focal lengths of the two analysers. The first slit is positioned at the calculated focal length of the energy monochromator. The second, post-collision slit also needs to be positioned on a common tangent to the radial ion trajectories within the two analysers. The slit assembly is somewhat novel in that it consists of two 180° opposite parallel slits on the walls of a hollow cylinder. When the cylinder is rotated on its axis, the ion beam entering perpendicular to the axis and slits "sees" variations of area overlap between the entrance and exit slits with the change of angle of rotation. Any slit width from zero to the maximum (1 mm in the present design) can be obtained under dynamic conditions by rotating the cylinder under vacuum by means of a Wilson seal.

The post-collision energy analyzer is followed by a channel electron multiplier detector which is located at the focal length of the second analyzer. The detector is operated in the particle counting mode and is interfaced through a fast amplifier to conventional pulse counting electronics and to a microprocessor controlled data acquisition system.

2.3 *Some operational characteristics*

Figure 5 shows a typical energy loss spectrum obtained when H_2^+ ions with 1.8 keV translational energy collide with N_2. This spectrum is an example of the application of TES to studies of excitation/de-excitation reactions depicted in figure 1 and

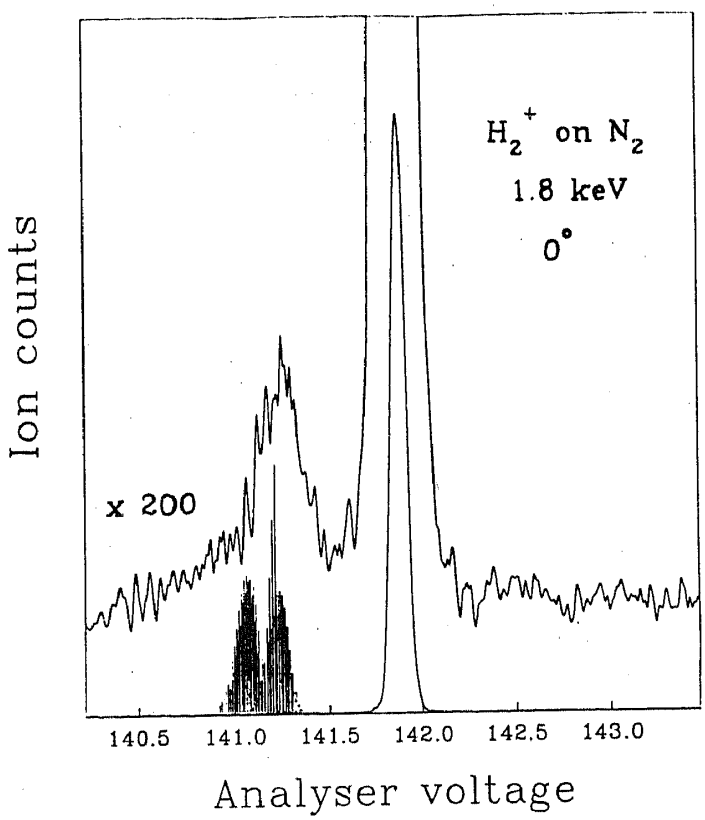

Figure 5. Translational energy spectrum of H_2^+ ions colliding with N_2 at 1·8 keV impact energy and 0° scattering angle. The peak in the vicinity of 142 V is the elastically scattered H_2^+ peak; the envelope of inelastic peaks in the region of 141·0 to 141·5 V are discussed in the text in terms of energy loss resulting from excitation of N_2 into various electronic states. The spectrum of vertical solid lines represents calculations of the transition probabilities for excitation to various N_2^+ excited electronic states.

represents the first such measurement of molecular target excitation induced by molecular projectile ion collisions reported to date. The elastically scattered H_2^+ ions give rise to the major peak in the spectrum; this peak has a full-width at half-maximum of 700 meV. This value represents an energy resolving power of just under 3000 which is obtained with ease and is adequate for purposes of illustrating the utility of the apparatus in studying collision-induced excitation processes involving singlet → triplet transitions which are forbidden by dipole selection rules.

The prominent peak observed at an energy loss of *ca.* 8 eV represents excitation of the target molecules in a composite process:

$$H_2^+ + N_2(^1\Sigma_g^+) \rightarrow H_2^+ + N_2^* - \Delta E \text{ eV}$$

where the N_2^{+*} states that are accessed are $A^3\Sigma_u^+$, $B^3\Pi_g$, $B'^3\Sigma_u^-$ and $a'^1\Sigma_u^-$. The relative transition probabilities for vertical excitation to each of these states from the ground state have been calculated by us using Franck–Condon factors obtained from the tabulated data of Lofthus and Krupenie [9]. The relative importance of each of these transitions in our spectrum is difficult to ascertain in a totally unambiguous fashion at present; a further, small enhancement in the resolving power is necessary and efforts are currently under way towards this end. For the purposes of this report, we wish to focus attention on the fact that this type of singlet-triplet excitation process

would, of course, be inaccessible in conventional photon spectroscopic techniques. In H_2^+–N_2 collisions, however, the possibility of electron exchange permits the multiplicity of the target molecule to change while the electron spin angular momentum of the ion-molecule system as a whole is conserved. Essentially 50% of all the bound electronic states of molecular species would be triplet states, or states of higher multiplicity. Such states have hitherto not been studied with the care afforded to singlet states because of the quantum mechanical restriction that for molecules with singlet ground states, states of higher multiplicity have optically forbidden decay transitions. Ion induced excitations studied by means of TES are clearly of much utility in this type of electronic spectroscopy. Resolving powers of the order of 5000 or more are sufficient to enable resolution of vibrational structure, and the first TES experiments on ion-induced "vibrational spectroscopy" has recently been reported by Mathur *et al* [10].

The energy loss spectrum shown in figure 5 is by way of illustration; a more detailed report on excitation of N_2 and O_2 molecules by ion projectiles possessing different quantal properties will be presented elsewhere [11]. However, it is to be noted that the projectile energy range over which the present apparatus can operate is 300 eV to 3 keV. This is exactly the energy range which is difficult to access in accelerator-based experiments (the lower translational energy limit in such experiments is seldom below 10 keV) as well as in ion swarm and other plasma type of experiments (where the highest energies that can be attained do not exceed 100 eV or so). Figure 6 shows the transmission function of the apparatus for H_2^+ ions produced under three different ion source and extraction conditions.

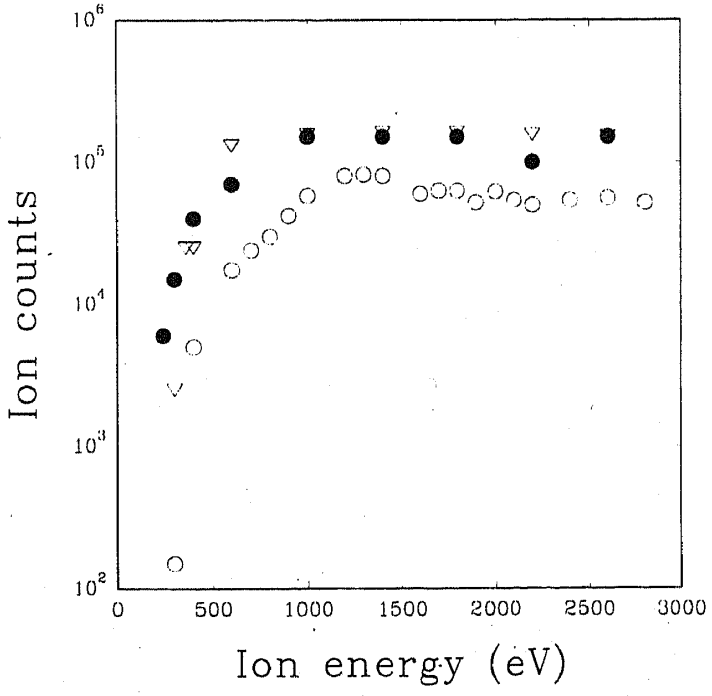

Figure 6. Transmission function for H_2^+ projectiles under different ion source conditions. Open circles: 3×10^{-6} torr; closed circles: 5×10^{-6} torr; triangles: 8×10^{-6} torr.

3. Collision-induced dissociation of CO_2^+ ions

Collision-induced dissociation of molecular ions may be understood in general terms as a two-step model within the framework of molecular potential energy surfaces. In the first step the projectile ion, AB^+, is collisionally excited to a higher electronic state:

$$AB^+ + M \rightarrow AB^{+*} + M - \Delta E.$$

In the second step, the ion in the excited state undergoes dissociation leading to the fragment ions:

$$\begin{aligned} AB^{+*} &\rightarrow A^+ + B + T_{cm} \\ &\rightarrow A + B^+ + T_{cm} \end{aligned}$$

A given excited state, AB^{+*}, may possess a potential energy (PE) curve which is either purely repulsive or the Franck–Condon transition from the ground state accesses that part of the PE curve which lies above the corresponding dissociation limit. A third alternative may involve an excited state which possesses a potential energy curve which has a minimum; such a state can undergo dissociation due to an avoided curve crossing involving a dissociative electronic state. This mode of

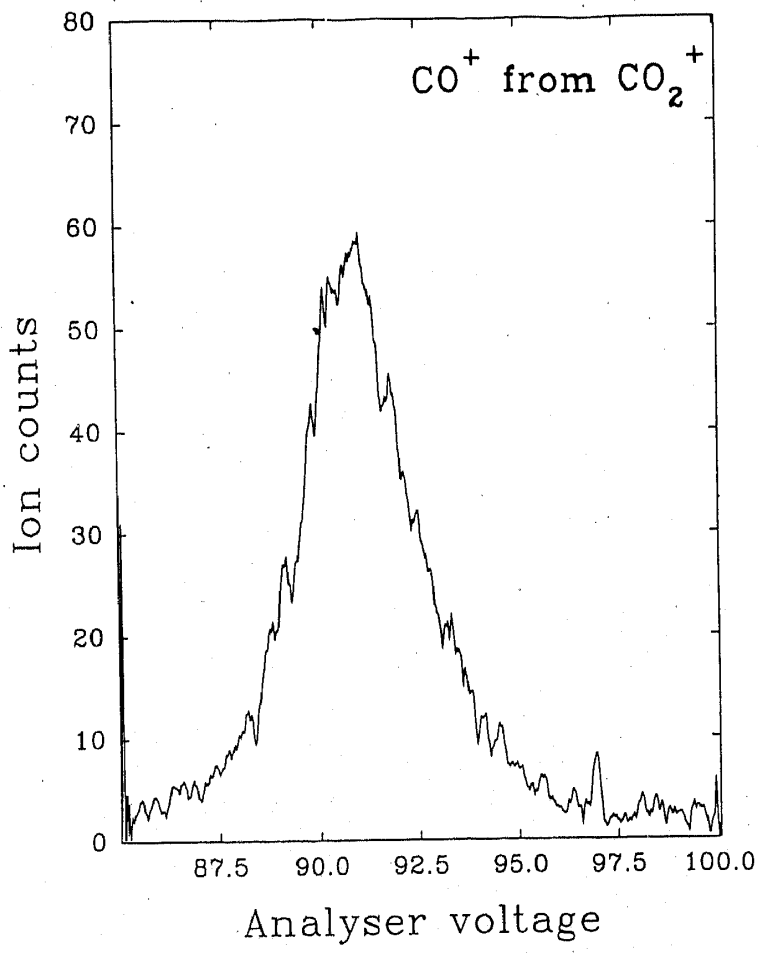

Figure 7. Translational energy spectrum of CO^+ fragment ions resulting from dissociation of CO_2^+ in 1·8 keV collisions with Ar.

dissociation is discussed below in the context of our results. The energy required for excitation, ΔE, in this inelastic process, is obtained by conversion of the projectile's kinetic energy into potential energy of the system.

Figure 7 shows a typical translational energy spectrum of CO^+ formed when CO_2^+ collides with neutral Ar at an impact energy of 1800 eV. Identical spectra are obtained when Ar is replaced by He or N_2 as the target gas. The projectile beam comprises mostly CO_2^+ in its ground $X^2\Pi_g$ state. As described in the two-step model the CO_2^+ molecule is initially excited to a higher electronic state which then dissociates to either $CO^+ + O$ or $CO + O^+$, releasing ε_{cm} energy in the centre-of-mass frame. This energy manifests itself as the kinetic energy of the fragment molecules and gives rise to the energy-broadened peak shown in figure 7 (compare with the energy width of the inelastic peak shown in the energy loss spectrum shown in figure 5). The measured energy in the laboratory frame, ε_{lab} can be obtained by the addition of collision velocities [1]:

$$\varepsilon_{lab} = \frac{M_{frag}}{M_{mol}} E + \frac{M_{frag}}{M_{mol}} \varepsilon_{cm} \cos^2\theta \pm \frac{M_{frag}}{M_{mol}} (\varepsilon_{cm} E)^{1/2} \cos\theta$$

where M_{frag} and M_{mol} are fragment and the projectile ion mass, respectively. θ is the angle of orientation of the molecular axis with respect to the beam axis and E is the energy of the projectile ion. Even though the numerical value of ε_{cm} may be small (of the order of a few hundred meV), ε_{lab} has a much larger value due to the addition of the velocity vectors. This energy 'amplification' which the TES method affords permits the study of the dissociation processes in considerable detail even with the instrument adjusted for modest energy resolution (and corresponding large ion intensities).

The $O^+ + CO$ dissociation channel was not measureable in our experiments, indicating that the excited electronic state of CO_2^+ that is initially accessed in the collision has quantal properties which give rise to only the $CO^+ + O$ dissociation limit. By measuring the half width of the CO^+ peak, we determine the average centre-of-mass kinetic energy release (KER_{cm}) value for the CO^+ fragment to be 170 ± 13 meV.

We correlate our energy spectrum of the CO^+ fragment to potential energy curves of CO_2^+ in the manner depicted in figure 8. CO_2^+ in its ground state ($X^2\Pi_g$) is collisionally excited to the $C^2\Sigma_g^+$ state. In the linear geometry this state correlates with CO^+ ($^2\Sigma^+$) + O (^{3}P), which is much above the C state. However the C state is predissociated by $^4\Pi_u$ state. So the dissociation of the molecule from the C state takes place through this quartet state. The CO_2^+ molecule in this state is more stable in the bent geometry, so it undergoes angular relaxation. At an OCO angle of 160° it undergoes another faster inter-system crossing to the X^2A_2 state, which corresponds to the $^2\Sigma_g$ state in the linear geometry. The molecule in the X state with large internal energy dissociates to $CO^+(^2\Sigma^+) + O(^3P)$ fragments.

Despite the apparent structural simplicity of the CO_2^+ molecular ion, there continues to be ambiguity regarding its proper quantal description. A number of high-level quantal calculations have been performed on the ground state and low-lying excited electronic states of this ion. In table 1 we draw attention to the divergent range of values of vertical excitation energy that have been computed for the $C^2\Sigma_g^+$ state as well as corresponding experimental data. Given that the C state is the electronic state that is responsible for formation of $CO^+ + O$ fragments, the amount of KER_{cm}

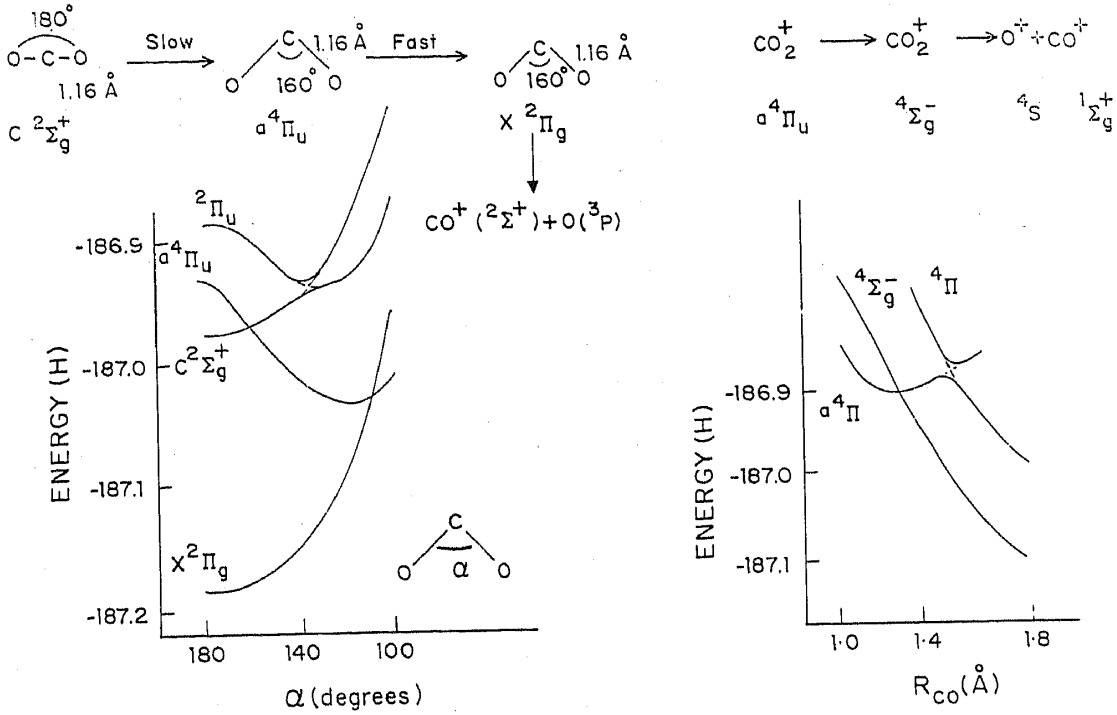

Figure 8. Schematic potential energy curves of low-lying excited electronic states of CO_2^+ (based upon the calculated results of Praet *et al* [13]) which take part in dissociation to $CO^+ + O$ fragments. The curves depicted on the left show variation of potential energy with the O–C–O angle; curves depicted on the right show the corresponding variation with C–O internuclear distance.

Table 1. Comparison of various contemporary values of the vertical excitation energy (in ev) of the $C^2\Sigma_g^+$ state of CO_2^+. All the values are results of large-scale ab initio calculation except the first which pertains to data from a He I photoelectron spectroscopy experiment.

Excitation energy	Reference
5·61	Potts and Fattahallah [12]
6·2	Roy *et al* [15]
5·69	Praet *et al* [13]
5·99	von Niessen *et al* [16]
5·49	Domcke *et al* [17]
7·25	England [14]
5·53	present work

obtained upon dissociation will be dependent upon the excitation energy: the larger the excitation energy, for a given (fixed-energy) dissociation limit, the larger will be the value of KER_{cm} that would be expected.

In view of the significant discrepancies that exist a calculation of the vertical excitation energy of the C state has been carried out by us using an all-electron, ab initio configuration interaction method [1, 2] with a 6-311G* basis set. Configuration interaction effects are accounted for by means of a coupled cluster formalism by a

computational method known as QCISD (T)[1, 2]. The vertical excitation energy of the C state from the X state is determined from our calculation to be 5·53 eV, in excellent agreement with the experimental value [12] and with the value calculated by Praet *et al* [13]. On the other hand, calculations carried out England *et al* [14] and Roy *et al* [15] yield significantly larger values of C state excitation energy. On the basis of our calculations, the C state in the Franck–Condon region is found to lie 140 meV above the $CO^+ (^2\Sigma^+) + O(^3P)$ fragments, in good accord with the average KER_{cm} value determined from our measured energy spectrum.

It is also of interest to note that the $^4\Pi_u$ state also crosses the $^4\Sigma^-$ state. The $^4\Sigma^-$ state correlates with $O^+(^4S) + CO(^1\Sigma^+)$ fragments. At low internal energies of the molecule in the C state (population of the lower vibrational levels of the C state) dissociation must necessarily be into $O^+ + CO$ fragments on purely energetic grounds. At higher energies (population of higher vibrational levels of the C state). the $CO^+ + O$ fragmentation channel becomes more dominant. Experimentally, we observe that the O^+ fragment is much lower in intensity (by about two orders of magnitude) than the CO^+ fragment. Our observation indicates that collisional excitation from the ground state leads to population of the higher vibrational levels of the C state.

Acknowledgements

We are grateful to B S Prahallada Rao and S R Halbe of the Technical Physics and Prototype Engineering Division of Bhabha Atomic Research Centre (Bombay) for their skilful assistance and advice in the high-accuracy machining of large (> 1m) diameter stainless rings during the fabrication of the two energy analysers. We also acknowledge S V K Kumar's assistance in preliminary computer simulation studies of ion trajectories in the ion source and extraction region.

References

[1] D Mathur, *Physics of ion impact phenomena*, (Springer-Verlag, Berlin, 1991)
[2] D Mathur, *Phys. Reports* **225**, 193 (1993)
[3] V Krishnamurthi, D Mathur and G T Evans, *Rapid Commun. Mass Spectrom.* **5**, 557 (1991)
[4] G R Kumar, L Menon and D Mathur, *Phys. Rev.* A (in press)
[5] D A Dahl, J E Delmore and A D Appelhans, *Rev. Sci. Instrum.* **61**, 607 (1990)
[6] M Szilagyi, *Electron Optics* (Plenum Press, New York, 1988) Ch. 3
[7] D Mathur, F A Rajgara and V Krishnamurthi, *Proc. Indian Acad. Sci* (*Chem. Sci.*) **104**, 509 (1991)
[8] F A Rajgara, *Ion translational energy spectrometry*, M.Sc. Thesis (University of Bombay, 1992)
[9] A Lofthus and P H Krupenie, *J. Phys. Chem. Ref. Data* **6**, 113 (1977)
[10] D Mathur, A C R Wilkins and A G Brenton, *Rapid Commun. Mass Spectrom.* **6**, 479 (1992)
[11] M Krishnamurthy and D Mathur-(in preparation)
[12] A W Potts and G H Fattahallah, *J. Phys.* **B13**, 2545 (1980)
[13] M Th. Praet, J C Lorquet and G Raseev, *J. Chem. Phys.* **77**, 4611 (1982)
[14] W B England, *J. Chem. Phys.* **77**, 6609 (1982)
[15] P Roy, I Nenner, P Millie, P Morin and D Roy, *J. Chem. Phys.* **84**, 2050 (1982)
[16] W von Niessen, G H F Diercksen and L S Cederbaum, *J. Chem. Phys.* **67**, 4124 (1977)
[17] W Domcke, L S Cederbaum, J Schirmer, W von Niessen, C E Brion and K H Tan, *Chem. Phys.* **40**, 171 (1979)